Changes in Thyroid Hormone Receptors After Permanent Cerebral Ischemia in Male Rats

Athanasios Lourbopoulos · Iordanis Mourouzis · Theodoros Karapanayiotides ·
Evangelia Nousiopoulou · Stavros Chatzigeorgiou · Theodoros Mavridis ·
Ioannis Kokkinakis · Olga Touloumi · Theano Irinopoulou · Konstantinos Chouliaras ·
Constantinos Pantos · Dimitris Karacostas · Nikolaos Grigoriadis

Abstract Thyroid hormones (TH) and receptors (TRs) may play an important role in the pathophysiology of acute cerebral ischemia. In the present study, we sought to determine whether serum triodothyronine (T3)/thyroxine (T4) and brain TRs (TRα1, TRβ1) might change after experimental stroke. Male adult Wistar rats were subjected to permanent middle cerebral artery occlusion (group P) and compared to sham-operated controls (group S). Animals were followed clinically for 14 days until brain collection for Western blot (WB) or neuropathological analysis of TRs in three different brain areas (infarcted tissue, E1; noninfarcted ipsilateral hemisphere, E2; and contralateral hemisphere, E3). Analysis of serum TH levels showed a reduction of T4 in group P ($p=$ 0.002) at days 2 to 14, while half of the animals also displayed "low T3" values ($p=0.012$) on day 14. This T4 reduction was inversely correlated to the clinical severity of stroke and the concomitant body weight loss ($p<0.005$). WB analysis of

TRα1 and TRβ1 protein expression showed heterogenic responses at day 14: total and nuclear TRα1 were similar between the two groups, while total TRβ1 decreased 7.5-fold within E1 ($p\leq0.001$) with a concomitant 1.8-fold increase of nuclear TRβ1 in E2 area ($p=0.03$); TRβ1 expression did not differ in E3. Neuropathological analysis revealed that activated macrophages/microglia exclusively expressed nuclear TRα1 within the infarct core. Astrocytes mildly expressed nuclear TRα1 in and around the infarct, along with a prominent TRβ nuclear signal restricted in the astrocytic scar. Neurons around the infarct expressed mainly TRα1 and, to a milder degree, TRβ. Surprisingly enough, we detected for the first time a TRβ expression in the paranodal region of Ranvier nodes, of unknown significance so far. Our data support that cerebral ischemia induces a low TH response, associated with significant and heterogenic changes in brain TR expression. These findings could imply an important role of TH signaling in cerebral ischemia.

Athanasios Lourbopoulos and Iordanis Mourouzis equally contributed to this work.

A. Lourbopoulos · T. Karapanayiotides · E. Nousiopoulou ·
S. Chatzigeorgiou · T. Mavridis · I. Kokkinakis · O. Touloumi ·
K. Chouliaras · D. Karacostas · N. Grigoriadis (✉)
B' Department of Neurology, Laboratory of Experimental Neurology
and Neuroimmunology, AHEPA University Hospital, Stilponos
Kiriakides str. 1, 54636 Thessaloniki, Macedonia, Greece
e-mail: grigoria@med.auth.gr

I. Mourouzis · C. Pantos
Laboratory of Pharmacology, Medical School, University of Athens,
75 Mikras Asias Ave, 11527 Goudi, Athens, Attiki, Greece

T. Irinopoulou
Institut National de la Santé et de la Recherche Médicale (INSERM),
Unité Mixte de Recherche en Santé 839, Paris, France

Introduction

Recent data suggest that thyroid hormones (TH) may play an important role in the pathophysiology of acute ischemic stroke. Human studies indicate that altered TH pattern is evident after cerebral ischemia and a reduction of serum triodothyronine (T3) appears to be associated with stroke severity and worse clinical outcome (Alevizaki et al. 2007; Zhang and Meyer 2010). Similarly, in a broader concept, changes in TH have been also associated with increased short-term mortality in the intensive care unit and with adverse

long-term outcome in cardiovascular disease (Golombek 2008; Mourouzis et al. 2011).

TH are important during the development of the mammalian brain (acting on multiple processes such as the migration and differentiation of neural cells, synaptogenesis, and myelination (Bernal 2007) as well as during the adult life (via a crucial role of thyroid receptors (TRs) on nervous system metabolism regulation, behavior, hippocampal/cerebellar function, and angiogenesis (Williams et al. 2007; Portella et al. 2010). TH mediate their actions through the activation of nuclear TRs that are transcription factors with ligand-regulated activity: in the absence of TH, the unliganded receptors (apo-receptors) recruit co-repressors and repress the transcription of target genes; upon hormone binding, the receptors (holo-receptors) exchange co-repressors for coactivators and activate transcription (Chassande 2003). TRs, namely the TRα and TRβ isoforms, are differentially and abundantly expressed in the normal and developing brain following a pattern of regional and cellular heterogeneity; the TRs are expressed in neurons, oligodendroglia, astrocytes, ependymal cells, and epithelial cells of the choroid plexus, with the most common isoform being that of TRα (Puymirat et al. 1991; Bernal 2007; Wallis et al. 2010). The "two-edge-sword" (apo- or holo-receptor state) function of TRs is always under the fine control of the available local thyroxine (T4)/triodothyronine (T3) levels resulting in fine-tuning of multiple genes (Di Liegro 2008).

Based on these data, the TH/TR system could be implicated in brain disease processes where damage of the central nervous system causes active recruitment of immature "repairing" cells and activation of "fetal" remodeling programs (Cramer and Chopp 2000), such as the case of stroke. In accordance with this concept, recent experimental studies have linked TH signaling with neuroprotection after ischemia via increase of neurotrophic factors and support of survival pathways (Genovese et al. 2013). Similarly, TH administration seems to be beneficial in experimental models of preterm intraventricular hemorrhage (Vose et al. 2013), neuronal trauma (Shulga et al. 2009), and neonatal hypoxia (Hung et al. 2013).

While several studies highlight multiple roles and functions for TRα1 and TRβ1 isoforms after ischemic injury of the heart (Pantos et al. 2010; Mourouzis et al. 2011), the role of TRs in the pathophysiology of adult ischemic brain injury remains largely unknown. Thereby, in the present study, we investigated whether changes in the TH/TR system can occur using an experimental model of ischemic stroke in rats. Most importantly, driven by the well-known role of TH and TRs for brain development, we focused on the remodeling phase of stroke as a period of high plasticity and reactivation of developmental gene programming

(Cramer and Chopp 2000). Deeper understanding of the role of TH signaling in the injured central nervous system may have potential important therapeutic implications.

Materials and Methods

Animal Handling and Experimental Groups

All experimental procedures were conducted according to institutional guidelines, in compliance with the Greek Regulations and the European Communities Council Directive 86/609/EEC. The study was conducted on male Wistar rats ($n=38$) of various weights (344–460 g). Rats were fed a regular diet and given water without antibiotics. Animals were randomly divided into two groups: group P ($n=29$) included animals that were subjected to permanent middle cerebral artery occlusion; group S ($n=9$) included sham-operated animals.

Permanent Middle Cerebral Artery Occlusion Model (p-MCAO)

The p-MCAO model was induced using operational procedures previously described in detail (Lourbopoulos et al. 2008; Lourbopoulos et al. 2012) additionally guided by a laser Doppler flowmetry (LDF) device (ML191 Blood FlowMeter, AD Instruments) (Harada et al. 2005). Briefly, rats were orally intubated and anesthesia was induced by 4 % and maintained with 1.5 % halothane in a mixture of 70 % N_2O and 30 % O_2 using mechanical ventilation (Small Animal Volume Controlled Ventilator—model 683—Harvard Apparatus). A LDF disk-probe (slightly modified MSP300XP miniature surface suturable probe, AD Instruments) was placed over the right hemisphere using the natural "pocket" between the lateral skull and the temporal muscle (Harada et al. 2005). The right middle cerebral artery (MCA) was permanently occluded using a poly-L-lysine-silicone-coated 5-0 suture (Lourbopoulos et al. 2008; Lourbopoulos et al. 2012), and LDF monitoring was maintained for approximately 20 min post-MCA occlusion. After the operation, the LDF probe was carefully and aseptically removed with restoration of the corresponding temporal muscle architecture.

Special care was paid during the p-MCAO operation for the least possible traumatic injury to the right thyroid lobe. Rectal temperature, mean arterial blood pressure (MABP), arterial blood gases, plasma glucose, and hematocrit values were also monitored during the operation. Postoperative intraperitoneal supplemental saline was administered where necessary. Mortality due to stroke was monitored, verified with autopsy, and measured as a clinical outcome.

Clinical and Motor Testing—Infarction Volume

All surviving animals were clinically examined and weighted on days 1, 2, 7, and 14 postoperatively. Clinical examination was performed using a seven-grade modified Bederson's Scale (mBS) (Lourbopoulos et al. 2008) and an 18-grade modified Neurological Stroke Scale (mNSS) (Zhang et al. 2002). Motor testing was performed using the grid walking test (GWT) (Rogers et al. 1997) and the relative videos were studied in slow motion to calculate the percentage of fault steps for each of the four limbs of the animals (Lourbopoulos et al. 2008). Using the differences of the animals' body weights per consequent days, we determined the percent change of body weight and the data were used as an indirect expression of a positive metabolic rate (pMR, increase of body weight) or negative metabolic rate (nMR, decrease of body weight).

Mean percent hemispheric infarction volume (%HVI) was calculated as previously described in detail (Lourbopoulos et al. 2008).

Blood Collection and Tissue Processing

Blood was aseptically collected from the femoral vein of the animals on days 2, 7, and 14 post-p-MCAO, under halothane anesthesia, with the aid of a stereoscope. Approximately 1.0 ml of whole blood was collected and serum was separated with a centrifuge at 3,000 rpm for 15 min. Serum was stored at −20 °C until further processing.

On day 14, animals were stratified for neuropathology ($n=7$) or Western blot (WB) analysis ($n=8$) of TRs and sacrificed under deep anesthesia. The former were transcardially perfused with 4 % paraformaldehyde (PFH), brains were removed, postfixed overnight in 4 % PFH, and processed for cryostat sections. The latter were decapitated, brains were quickly removed, cut into three different areas (E1: infarction area, E2: noninfarcted right hemisphere, and E3: left hemisphere; Fig. 2d), snap-frozen into liquid nitrogen, and stored at −80 °C until further processing. The corresponding areas were also collected from group S.

T3 and T4 Quantification

Plasma ʟ-thyroxine (T4) and 3,5,3′ tri-iodothyronine (T3) quantitative measurements (nmol/l) were performed with ELISA (Alpha Diagnostic International, TX, USA; No 1100 for total T4 and No 1700 for total T3) (Pantos et al. 2005). Absorbance measurements were performed at 450 nm with Tecan Genios ELISA reader (Tecan, Austria).

Determination of TRα1 and TRβ1 Protein Expression Using Western Blotting

Brain tissues from E1, E2, and E3 areas were homogenized in ice-cold buffer (A) containing 10 mM 4-(2-hydroxyethyl)-1-piperazineethanesulfonic acid (HEPES; pH 7.8), 10 mM KCl, 0.1 mM ethylenediaminetetraacetic acid (EDTA), 0.1 mM ethylene glycol tetraacetic acid (EGTA), 0.5 mM phenylmethyl sulfonyl fluoride (PMSF), 1 mM dithiothreitol (DTT), and 10 μg/ml leupeptin. Two hundred microliters of 10 % Igepal was added and samples were left in ice for 30 min. Homogenization was repeated and a small fraction of total lysis was kept for further analysis. The rest of the homogenate was centrifuged at $1,000 g$ for 5 min at 4 °C, and the pellet containing the nuclear fraction was washed again in buffer (A) with 1 % Igepal. The final pellet was resuspended in buffer (B) containing 20 mM HEPES (pH 7.8), 420 mM NaCl, 1 mM EDTA, 1 mM EGTA, 0.5 mM PMSF, 1 mM DTT, 10 μg/ml leupeptin, and 10 % glycerol, and samples were incubated at 4 °C for 60 min (under agitation) followed by centrifugation at $10,000 g$ for 5 min at 4 °C. The supernatant containing the nuclear fraction was separated and stored at −80 °C, while the pellet containing cellular debris and cytoskeleton was discarded. TRα1 and TRβ1 protein expression was determined in total and in nuclear fraction. Protein concentrations were determined by the BCA method.

Samples were prepared for sodium dodecyl sulfate polyacrylamide gel electrophoresis (SDS-PAGE) by boiling for 5 min in Laemmli sample buffer containing 5 % 2-mercaptoethanol. Two hundred micrograms (nuclear fraction) and 40 μg (total lysis) of total protein were loaded onto 10 % (w/v) acrylamide gels and subjected to SDS-PAGE in a Bio-Rad Mini Protean gel apparatus. For Western blotting, following SDS-PAGE, proteins were transferred electrophoretically to a nitrocellulose membrane (Hybond ECL) at 100 V and 4 °C for 1.5 h using Towbin buffer. After Western blotting, filters were probed with specific antibodies against TRα1 and TRβ1 (Affinity Bioreagents, MA1-216, dilution 1:1,000, o/n at 4 °C). In order to normalize variations in protein loading, filters of nuclear fraction were probed with histone H3 antibody (Cell Signaling, #9715, dilution 1:1,000, o/n at 4 °C), while filters of total fraction were probed with a-actin antibody (Sigma, dilution 1:1,000, o/n at 4 °C). Filters were incubated with appropriate anti-mouse (Amersham) or anti-rabbit (Cell Signaling) HRP secondary antibodies, and immunoreactivity was detected by enhanced chemiluminescence using Lumiglo reagents (New England Biolabs) and exposed to Hyperfilm paper (Amersham). Five samples from each group were loaded on the same gel. TRs were expressed as the ratio of TRα1 and TRβ1 band density to H3 or actin band density in nuclear or total fraction, respectively. Immunoblots were quantified using the AlphaScan Imaging Densitometer (Alpha Innotech Corporation, 14743, Catalina Street, San Leandro, CA).

Double Immunofluorescence and Neuropathology

Localization of TRα1 and TRβ signal was studied using double immunofluorescence (dIF) on 10 μm cryostat coronal brain sections. Following hydration, a short cycle of mild antigen retrieval (pH 6, 10 min in hot citrate buffer) and incubation of the sections with 10 % fetal bovine serum (FBS) for 30 min, primary antibodies were applied overnight. The following combinations of primary antibodies were studied: TRα1 (1:200, rabbit polyclonal, Acris) or TRβ (1:100, rabbit polyclonal, Acris) with (a) Mac-3 (1:500, mouse, BD Biosciences) for macrophages, (b) Iba1 (1:400, goat polyclonal Abcam) for macrophages/microglia, (c) CNPase (1:400, mouse monoclonal, Millipore) for myelin, (d) NeuN (1:200, mouse monoclonal, Millipore) for neurons, (e) GFAP (1:100, mouse monoclonal, DAKO) for astrocytes, (f) neurofilament-H SMI-31 (1:800, mouse monoclonal, Calbiochem) for axons, and (g) Caspr (1:300, mouse monoclonal, Abcam) for paranodal characterization. Depending on the primary antibodies used, sections were incubated with the following secondary fluorescent antibodies: goat or donkey anti-rabbit IgG (Biotium 488) for TRα1 or TRβ and goat anti-mouse or donkey anti-goat IgG (Biotium 555) for the rest of the markers. Nuclei were counterstained with DAPI (Biotium) and mounted with the corresponding Biotium mounting medium. Sections were studied using a Nikon (Eclipse C1 Plus TE2000-U) or a Leica (SP7) confocal inverted microscope.

Quantification of TRα1 and TRβ expression in the tissue was performed with the aid of FIJI/ImageJ 1.46j software (NIH software) on two to four sections, spaced at least 100 μm apart. The stained sections (as described above) were studied under ×63 optical fields at the following three areas: the infarct core and scar (e1 area), the close peri-infarct area (+ 100 μm distance from the scar border, area e2), and the healthy contralateral corresponding hemisphere (area e3); area e3 was used as internal control. Five images were captured per area per animal and the total TRα1 or TRβ expression was measured as "Integrated Density" using the ImageJ software, as previously described (Theotokis et al. 2012). Data were expressed as arbitrary density units (IntDen), representing area and signal intensity. In addition, the same images were used to evaluate the percentage of cells expressing each one of the two TR isoforms in their nucleus; data per each cell type are presented as mean percentage values per high power field. Finally, studies of colocalization and 3D reconstruction of the TRβ expression in the nodes of Ranvier were performed using the Imaris Software on confocal z-stack images.

Antibody Preabsorption Assay

Verification of the antibody specificity was performed with a preabsorption assay using the corresponding control peptide

(Acris), according to the manufacturer's instructions and protocol. Briefly, the peptide was mixed with the antibody in a 72× molecular ratio and was incubated under gentle agitation in room temperature for 30 min. The mixture was then used in place of the primary antibody for the rest of the IF protocol, as described. Thus, three identical brain sections were used, each of which was incubated with (a) the primary TRβ antibody (regular IF), (b) the preabsorbed TRβ antibody with the corresponding peptide, and (c) incubation only with the secondary Biotium 488 antibody. Sections were mounted with a DAPI containing mounting medium (Biotium). Pictures were taken under an epifluorescent microscope.

Statistical Analysis

All data are given as mean ± standard error. Statistical analysis was performed using the SPSS 18.0 package. Student's t test and Mann-Whitney U test or one-way ANOVA (with LSD post hoc test) were used, where appropriate, for comparisons of scale data. The possible relations between different parameters were investigated using Pearson correlation coefficients. Repeated measures general linear modeling was used for the analysis of serial data obtained from the same animals. Two-tailed values of $p < 0.05$ were considered significant for all tests.

Results

Physiological Variables

All measured physiological variables remained within normal limits pre- and postoperation ($p > 0.05$, one-way ANOVA). During anesthesia, rectal temperature was maintained at 37.0 ± 0.1 °C without intraoperative cooling. Intraoperative LDF monitoring showed successful MCA occlusion in all group P animals. Mortality due to severe stroke occurred in 14/29 of group P animals, as was verified at autopsy. Subarachnoid hemorrhage was not observed in any of the animals.

Initial, preoperative, body weight was similar in both groups (S, 424.0 ± 12.6 g versus P, 395.5 ± 8.2 g; $p > 0.05$). Postoperative weight loss (nMR) occurred in both animal groups in 24 h and day 2 (Fig. 1a), and this was partially attributed to previously reported postoperative complications of MCAO surgery (Dittmar et al. 2003; Dittmar et al. 2005). However, group P exhibited a higher nMR in 24 h (P, -7.2 ± 0.6 % versus S, -3.3 ± 0.3 %, $p = 0.0001$; Fig. 1a) and continued to lose weight even after day 7 resulting in constant nMR up to day 14 (P, -7.5 ± 2.6 % versus S, 4.1 ± 1.6 %, repeated measures analysis, $p = 0.003$; Fig. 1a). These changes of body weight during days 7 and 14 were strongly correlated with the stroke severity as was expressed through the mNSS score on
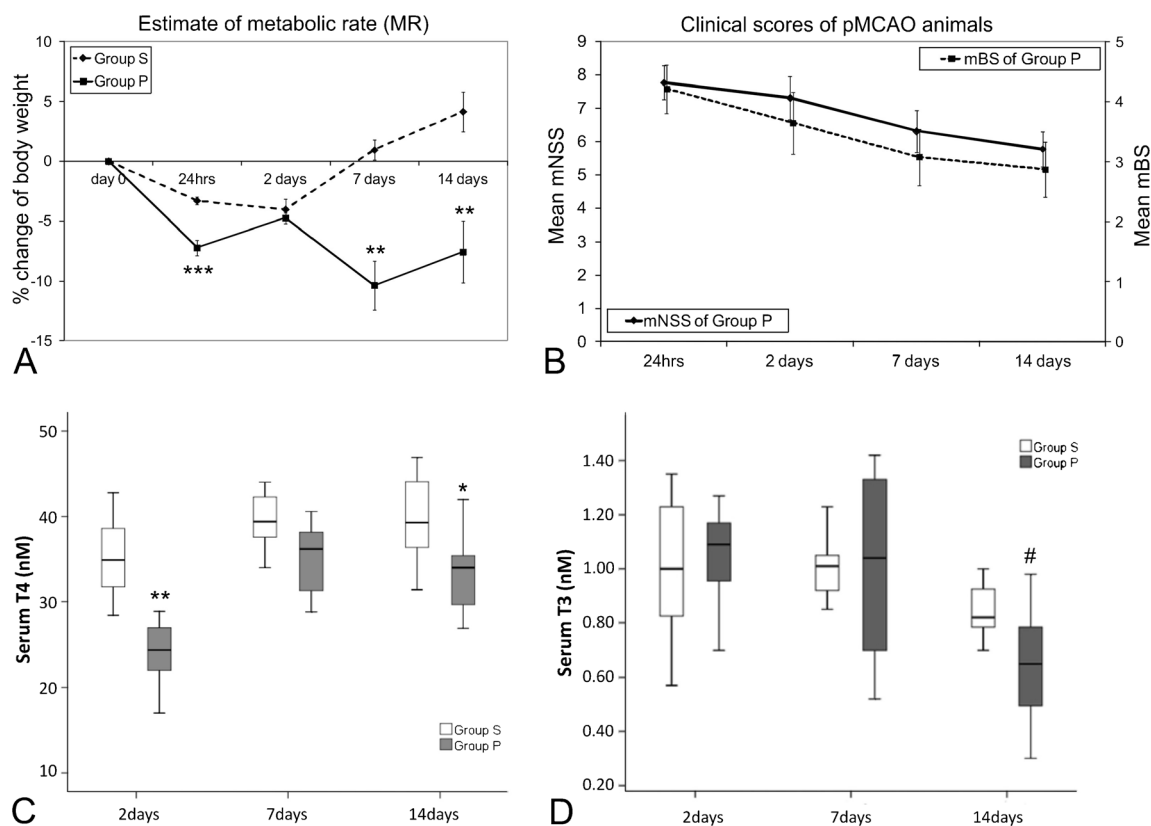
Fig. 1 Animal clinical characteristics during the 14-day follow-up period. **a** Estimate of the metabolic rate (MR) of the animals expressed as a mean % change of body weight. **b** Mean mNSS (*left vertical axis*) and mBS (*right vertical axis*) clinical scores of group P. **c, d** A box-whiskers plot of the serum T4 and T3 levels after ischemia (median and quartiles, whiskers indicate ±1.5 interquartile range). *$p<0.05$, **$p<0.01$, ***$p<0.001$; #$p<0.05$ for paired t test between day 2 and day 14 for group P

day 1 (Pearson's $r=-0.796$ and -0.644, $p=0.0004$ and $p=0.01$, respectively, for days 7 and 14).

Neurological Deficits and Cerebral Infarction Volume

The group P animals developed ischemic stroke with mNSS and mBS scores displayed in Fig. 1b (day 1 mNSS=7.8±0.5 and mBS=4.2±0.4). The % left forelimb fault steps (affected limb) on GWT were on day 1, 64.8±3.0 %; on day 2, 66.8±5.5 %; on day 7, 50.6±5.2 %; and on day 14, 59.8±7.1 %. Animals of group S did not exhibit any neurological deficit at any time point. On day 14, the mean %HVI was 14.76±2.73 % for group P and hemispheric edema was not detected.

Serum T3 and T4 Levels

Levels of T3 and T4 at 2, 7, and 14 days are shown in Fig. 1c, d. T4 levels were reduced in group P on day 2 (group P, 22.6±2.8 nM versus group S, 35.3±2.0 nM; $p=0.007$), day 7 (group P 34.7±1.6 nM versus group S, 39.0±1.8 nM; $p=0.097$), and day 14 (group P, 31.9±2.5 nM versus group S, 39.8±2.1 nM; $p=0.034$); repeated measures analysis revealed that the

observed T4 reduction in the group of permanent ischemia was significant ($p=0.002$) when compared to the sham-operated group. In addition, the decreased T4 levels on day 2 were inversely correlated to the mNSS score at 24 h and day 2 post-ischemia (Pearson's $r=-0.766$ and -0.789; $p=0.002$ and 0.001, respectively), meaning that more severe (clinically) strokes were associated with a lower T4 serum level. In the same context, the low T4 levels on day 2 (Pearson's $r=0.767$, $p=0.002$) were strongly associated with the body weight reduction (nMR) on day 7, providing evidence for a possible relation of the low T4 levels on the body weight reduction seen after stroke.

The serum T3 levels, overall, did not statistically differ between the two groups during the post-ischemic period examined (repeated measures analysis, $p=0.883$). However, in group P at 14 days, approximately 50 % of the values were lower than the lower T3 limit in group S ("low T3" values). Furthermore, the 14-day T3 levels in group P were decreased compared to the corresponding levels at 2 days (for day 2, 1.03±0.08 nM versus day 14, 0.64±0.9 nM; $p=0.012$; Fig. 1d) and strongly correlated with the body weight on day 14 (Pearson's $r=0.653$, $p=0.011$). These changes are in alignment with the corresponding T4 changes.

TRα1 and TRβ1 Protein Expression in Different Brain Areas Using Western Blotting

The protein expression of TRα1 on day 14 was similar between the two groups in the three brain areas studied (Fig. 2), although a trend for reduced nuclear TRα1 was detected in the infarction area of group P (Fig. 2a, $p = 0.1$).

Conversely, TRβ1 expression on day 14 was different among the three brain areas studied (Fig. 3). Total expression of TRβ1 was found to be 7.5-fold less in the infarct area (E1, $p \leq 0.001$, Fig. 3a), while no difference was observed in the peri-infarct (E2) and remote (E3) regions of group P compared to group S ($p > 0.05$, Fig. 3b, c). Furthermore, nuclear expression of TRβ1 was found to be 3.5-fold less in the infarct area (E1, $p = 0.01$) and 1.8-fold higher in the peri-infarct region

(E2, $p < 0.03$), while no difference was observed in the remote (E3) region of group P compared to group S ($p > 0.05$).

Localization of TRα1 and TRβ Protein Expression in the Brain Using Neuropathology

Confocal microscopy revealed spatial differences in the expression pattern of TRα1 and TRβ on day 14, as expressed by Integrated Density analysis (Fig. 4a, b). TRα1 expression was similar among the three brain areas studied, despite a trend for increased TRα1 expression in the infarction core compared to the peri-infarct area ($p = 0.08$, Fig. 4a). Conversely, TRβ expression was greatly reduced in the infarct core compared to the peri-infarct area (Fig. 4b).
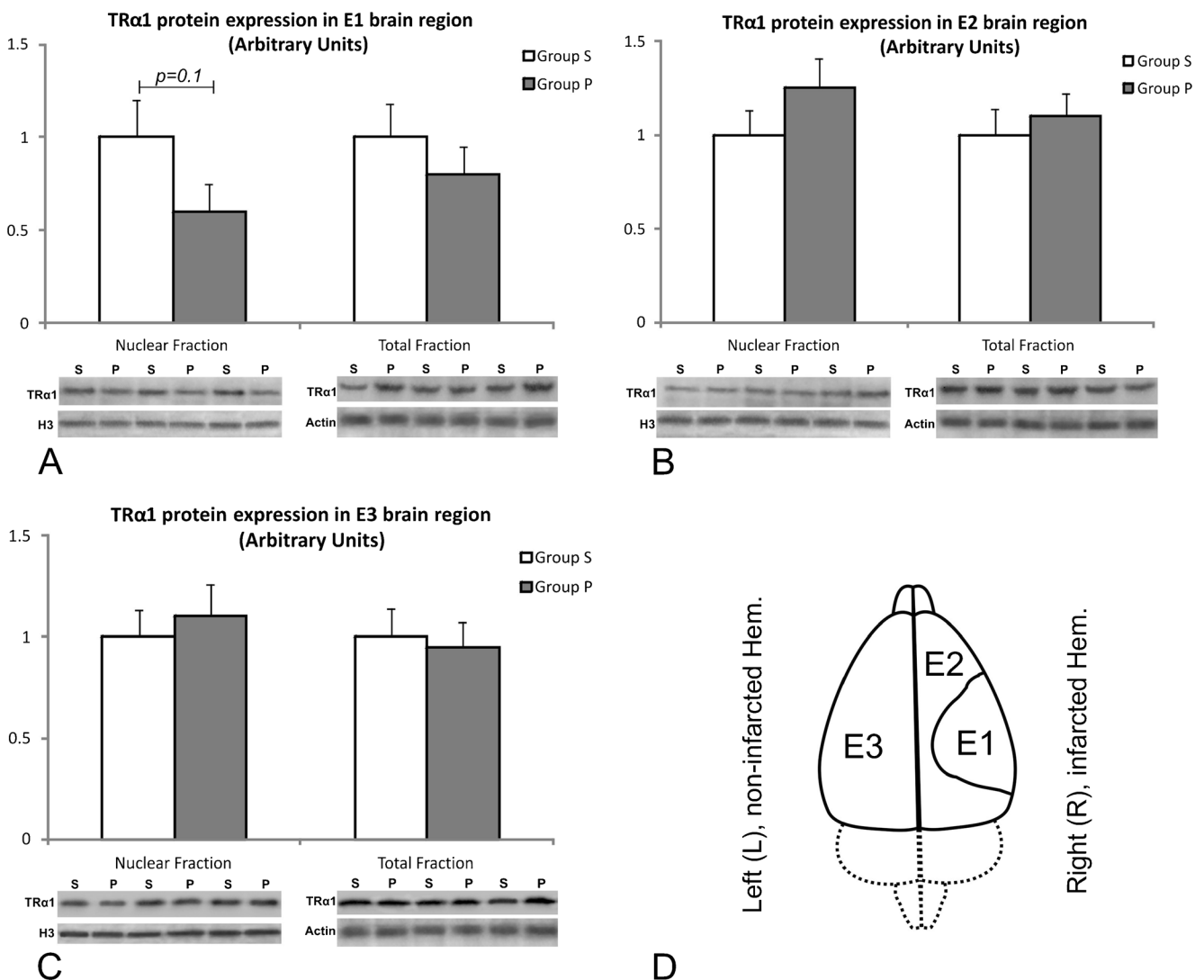
Fig. 2 Densitometric assessment (in arbitrary units) of TRα1 protein expression (total and nuclear fraction, WB analysis) in the three brain areas (E1–E3) of groups P and S (*bars* indicate means±s.e.m. of the corresponding optical ratios). Representative Western blots of TRα1 and the corresponding loading controls (H3 for nuclear fraction or actin for total fraction) are shown below each of the graphs **a**–**c**: there is only a trend for lower nuclear TRα1 expression in the infarction area (E1) of group P, while areas E2 and E3 exhibit no differences. **d** Graphical illustration of the brain areas studied with WB (E1: infarction, E2: peri-infarct area, E3: noninfarcted hemisphere)
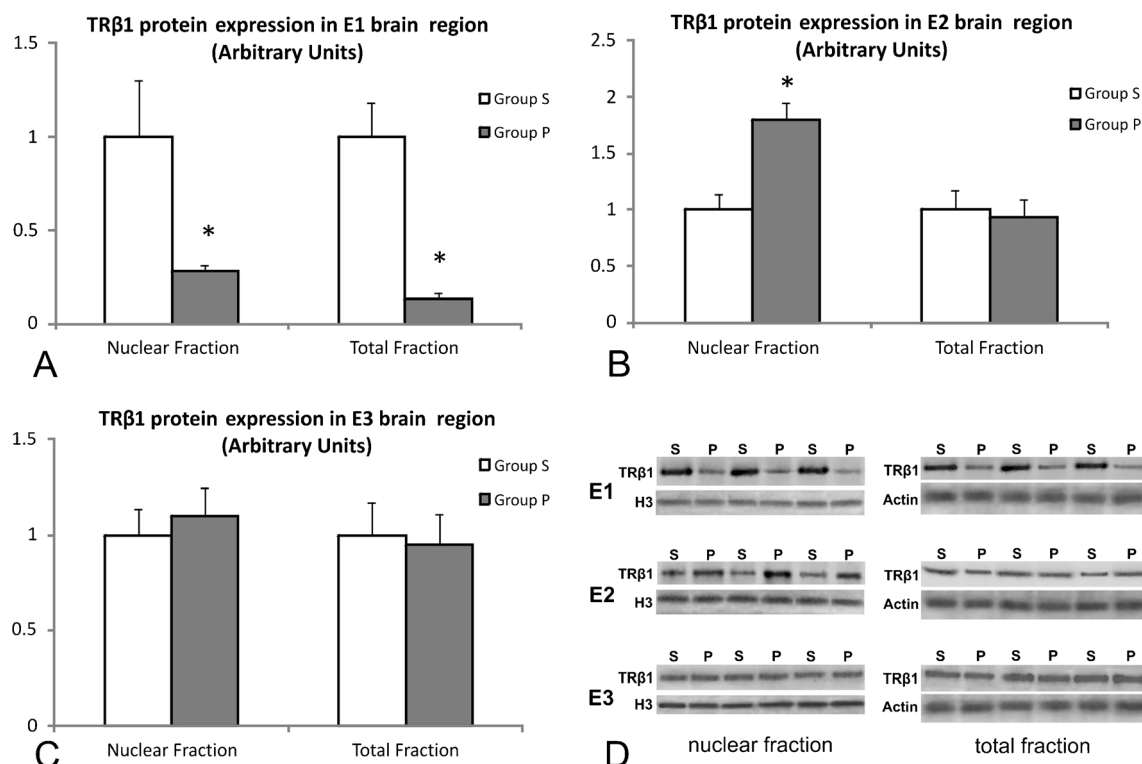
Fig. 3 Densitometric assessment (in arbitrary units) of TRβ1 protein expression (total and nuclear fraction, WB analysis) in the three brain areas studied (E1–E3, *bars* indicate means±s.e.m. of the corresponding optical ratios). Graphs **a–c** show a significant reduction of TRβ1 in infarction (E1 area), along with a relative increase of nuclear TRβ1 in area E2; no changes were present in area E3. **d** Representative TRβ1 WB lanes along with the corresponding loading controls from nuclear and total fractions of groups S and P. *$p<0.01$

Further detailed analysis showed that TRα1 was heterogeneously expressed in different cell types. Neurons in cortical and subcortical structures (neocortical layers II/III and VI, piriform cortex, hippocampus, hypothalamus, thalamus, and striatum) were TRα1+, in agreement with previous reports (Wallis et al. 2010), except the infarction core where few—if any—neurons were present (Fig. 5a–c). In the peri-infarct area (e2), 71.8±3.6 % of NeuN + cells expressed a nuclear TRα1, whereas in area e3, the nuclear TRα1 signal was detected 39.6±7.3 % of the NeuN + cells ($p=0.0003$, Fig. 4c). The majority of the astrocytes expressed a weak nuclear TRα1 (91.1±2.2 %) in the infarct scar (e1) and the proximal peri-infarct area (86.1± 2.9 %, $p=0.361$). The majority of "resting" astrocytes in e3 were TRα1 negative (4.1±1.3 %, Figs. 4d and 5d–f). Oligodendrocytes constantly expressed TRα1 (both nuclear and cytoplasmic expression) within the gray and white matter, with no significant differences among the three brain areas studied (e1–3, Fig. 4e); within the infarction core and peri-infarct scar, scarce oligodendrocytes were only present without any difference in TRα1 expression (Figs. 4e and 5g–i2). Axons (SMI31 positive) were TRα1-negative (Fig. 5j–l). Within the infarction core, macrophages/amoeboid microglia or foam cells (Iba1+ cells) ubiquitously expressed TRα1 in their nucleus (Figs. 4f and 5m). Outside of the infarction, all resting or ramified microglia (Iba1+) in the rest of the brain (areas e2 and e3) were TRα1 negative (Figs. 4f and 5n, o).

TRβ was also expressed on neurons in areas e2 and e3, although its signal was weaker than TRα1, whereas the infarction core (area e1) was devoid of any neurons (Figs. 4c and 6a–c). In these areas, 56.7±6.9 % (e2) and 7.7±3.1 % (e3) of NeuN + cells exhibited a nuclear TRβ signal ($p<0.0001$). Astrocytes were TRβ negative in the peri-infarction area (e2, Fig. 6e) and the noninfarcted hemisphere (area e3, Fig. 6f), but the majority of them expressed a strong TRβ nuclear signal in the astrocytic scar (89.8±2.6 %, Figs. 4d and 6d). Oligodendrocytes were ubiquitously TRβ+ in areas e2–e3 (Fig. 6h–j(2)) and area e1 (although few CNPase+ cells could be detected in the infarction). Axons were negative for TRβ in all areas studied (Fig. 6k–m(2)). Interestingly and in contrast to TRα1, all Iba1+ cells were TRβ negative within the infarction core (Figs. 4f and 6n); we could only detect a few foci of cytoplasmic TRβ signal within phagocytes (insert in Fig. 6n), which could be phagosomes of unknown composition. Resting or ramified microglia in the e2 and e3 areas similarly did not express TRβ (Fig. 6o, p). Overall, the expression and localization of TRα1 and TRβ in relation to the different cell types studied is summarized in Fig. 7.

Total TRα1 and TRβ expression in areas e1-3 (Integrated Density)
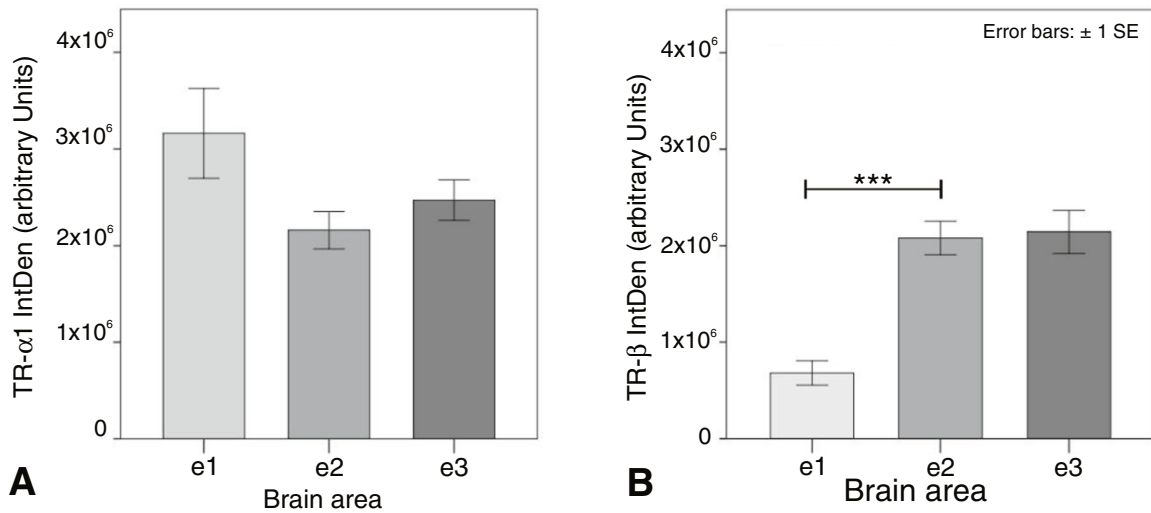
Nuclear localization of TRs in each cell type (% of cells)
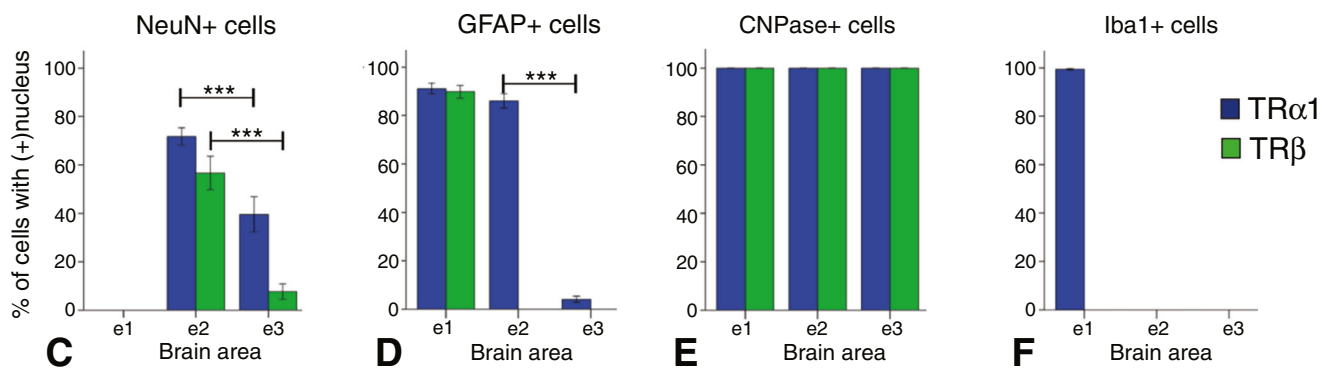
Fig. 4 Quantification of TRs expression. Total TRα1 and TRβ expression in brain areas e1, e2, and e3 (arbitrary units of "IntDen," mean ±s.e.m.) is shown in graphs **a** and **b**, respectively. The percentage of cells expressing TRs in their nucleus (mean±s.e.m.), per brain area, is shown in graphs **c** (NeuN+, neurons), **d** (GFAP+, astrocytes), **e** (CNPase+, oligodendrocytes), and **f** (Iba1+, macrophages/microglia). ***$p<0.001$

### Localization of TRβ but not TRα1 in the Paranodal Area of Ranvier Nodes

Interestingly enough, a consistent TRβ expression was observed in the myelinated white matter tracts of the brain as a repeated pattern of "paired-dotted" signal (Figs. 6i(2), j(2), and 8), interrupted by a space of approximately 1 μm between dots, which is in accordance with the Ranvier node width (Zoupi et al. 2011). This signal was ubiquitously co-expressed with myelin in the corpus callosum and cortex (CNPase+, Fig. 6i(1), j(2)) and was adjacent to axons (SMI31+ axons, Fig. 6l(1), m(2)). Double IF for Caspr (paranodes) indicated that TRβ was co-expressed in the paranodal region of Ranvier nodes (Fig. 8a, b). In addition, 3D reconstruction studies revealed that TRβ expression

extended for 1–2 μm within the juxta-paranodal area of the myelin sheath (Fig. 8c, d). This localized expression of TRβ in the paranodal region followed the general expression pattern of TRβ (reduced in the infarction core, no differences in areas e2 and e3, data not shown). Preabsorption of the TRβ antibody with its antigenic peptide abolished its signal in both paranodal areas and brain cells, as shown in the Supplementary figure, further supporting the specificity of our data.

Discussion

Our results indicate that TH signaling is altered after experimental cerebral ischemia. TH levels are reduced for at least 2 weeks after focal ischemic stroke and the relevant TRs are
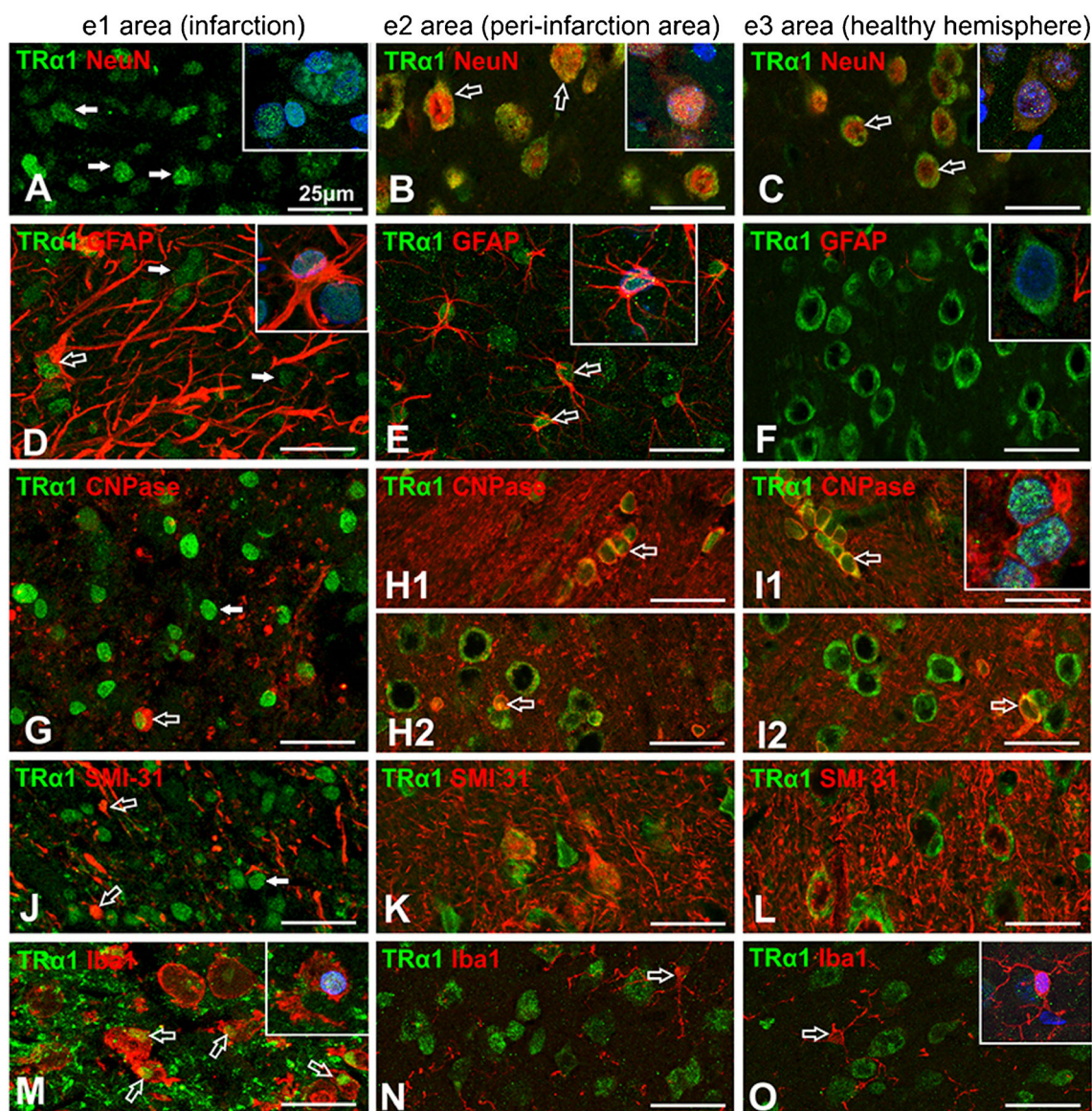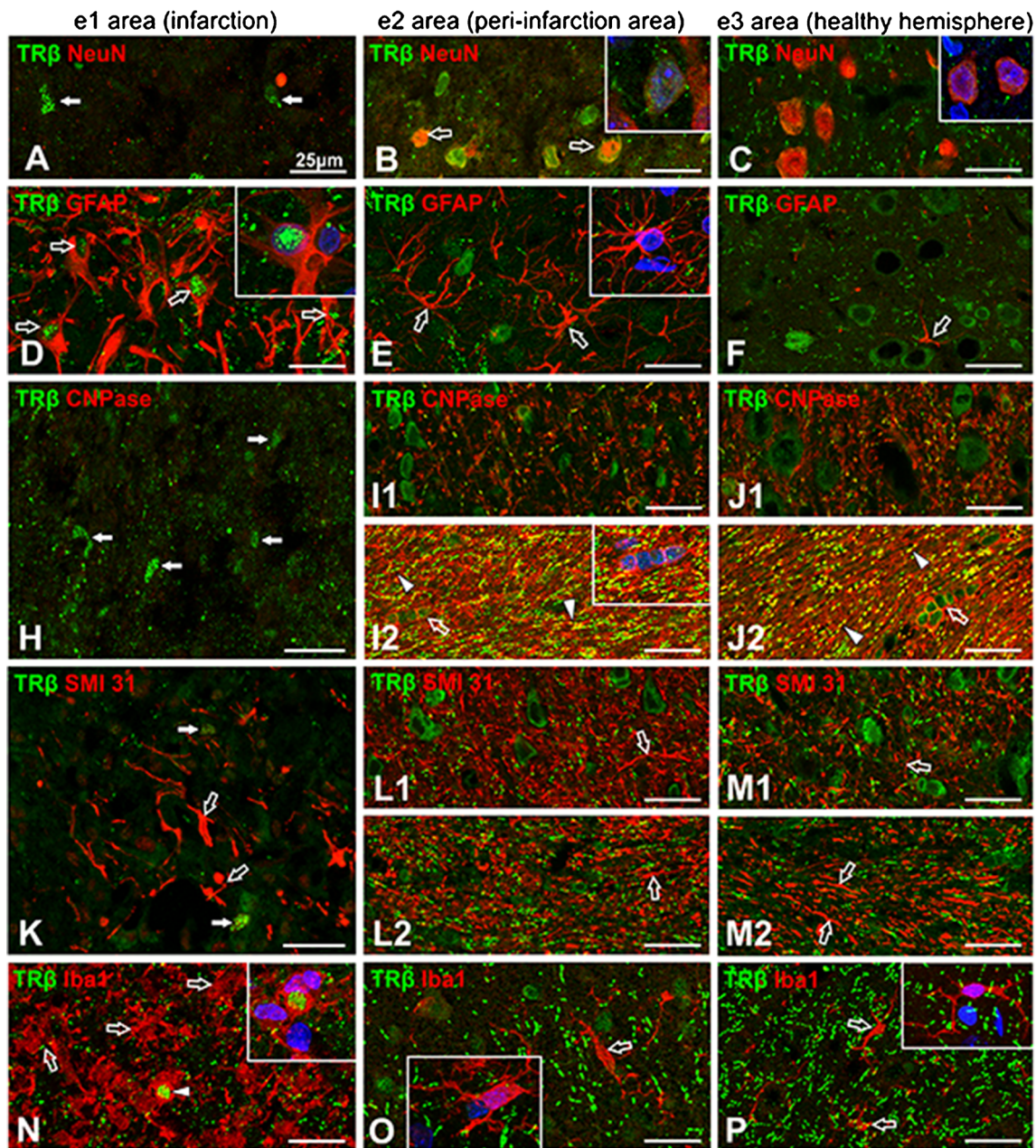
Fig. 5 Confocal microscopy study of TRα1 expression. Neurons (NeuN+, *open arrows*) are absent from e1 (**a**) and express TRα1 in their nucleus mainly in e2 (**b**, *insert*) and less in e3 (**c**, *insert*; for exact quantifications, see text). Astrocytes (GFAP+, *open arrows*) express nuclear TRα1 in areas e1–2 (**d**, **e**, *inserts*) but not e3 (**f**, *insert* shows an astrocytic process next to a TRα1+ cell). Oligodendrocytes and myelin (CNPase+, *open arrows* point at oligodendrocytes positive for TRα1; **h**(*1*) and **i**(*1*) in corpus callosum, **h**(*2*) and **i**(*2*) in cerebral cortex; *insert* in **i**(*1*) shows oligodendrocytes with TRα1+ nucleus). **j**–**l** Axons (SMI31+, *open arrows* in **j** point at injured axons-ovoids). **m**–**o** Microglia/macrophages (Iba1+, *open arrows* point at TRα1+ macrophages/microglia in **m** and at TRα1 negative microglia in **n**, **o**). *Inserts* show magnification of representative DAPI + cells (*blue*) in each panel. *White arrows* indicate TRα1+ nuclei. *White scale bars*=25 μm

differentially implicated in the local tissue processes in and around the ischemic infarct. TRα1 is preferentially expressed by macrophages and TRβ by reactive astrocytes within the infarction, 14 days after ischemia. At the same time, neurons around the infarct exhibit increased nuclear localization of TRs (mainly TRα1). Finally, we surprisingly detected for the first time a novel localization of TRβ in the paranodal/juxta-paranodal area of Ranvier nodes in the rat brain, with unknown function and relevance so far.

A post-ischemic decline in serum T4 levels is already evident acutely post-ischemia. This decline remains up to 14 days and is also associated with late "low T3" values in half of the animals. The present findings are in accordance with previous clinical studies that reported low TH levels in stroke patients (Alevizaki et al. 2007; Zhang and Meyer 2010). Low levels of TH seem to be protective after stroke, as indicated by recent clinical observations (Akhoundi et al. 2011; Wollenweber et al. 2013). However, the significance of TH reduction after stroke is yet not fully known. It could represent a "reflex" response of the tissue/organism to protect itself from the low-oxygen (low-energy) state (Diano and Horvath 2008; Simonides et al. 2008) or even a response to

Fig. 6 Confocal microscopy study of TRβ expression. Neurons (NeuN+) are absent from e1 (**a**) and express TRβ mainly in e2 (**b** and *insert*, *open arrows*, nuclear expression); astrocytes (GFAP+) strongly express TRβ in their nuclei in the astrocytic scar (**d**, *insert*, *open arrows*) but not in e2 or e3 (**e**, **f**, *insert*, *open arrows*). **h**–**j**(2) Oligodendrocytes and myelin (CNPase+, *open arrows* point at TRβ + oligodendrocytes: **i**(1) and **j**(1) in cortex, **i**(2) and **j**(2) in corpus callosum; *arrowheads* in **i**(2) and **j**(2) point at CNPase+/TRβ + formations in the white matter, see also Fig. 8).

k–**m**(2): axons (SMI31+, *open arrows* point at TRβ-negative axons: **l**(1) and **m**(1) in cortex, **l**(2) and **m**(2) in corpus callosum). **n**–**p** Microglia/macrophages (Iba1+, *open arrows* point at TRβ-negative macrophages/activated microglia in **n** and at ramified/resting microglia in **o**, **p**; *arrowhead* in **n** points at a cytoplasmic focus of TRβ). *White arrows* in **a**, **h**, and **k** point at TRβ + nuclei. *Inserts* show magnification of representative DAPI + cells (*blue*) in each panel. *White scale bars*= 25 μm

the "aseptic" inflammation after ischemia as part of the "nonthyroidal illness syndrome" (Boelen et al. 2011). However, a sustained hypothyroid state observed after stroke seems to delay rather than actually prevent neuronal death (Lee et al. 2010); in accordance to this, acute T4 administration after stroke seems to be beneficial, at least during the first

24 h (Genovese et al. 2013). On the other hand, the association of TH with the catabolic state of the animals (sarcopenia) observed after MCAO may seem partially contradictory. Hypothyroidism is usually associated with a gain of weight as well as low-energy consumption (Mistry et al. 2009), yet sarcopenia after MCAO could probably be explained at least

Fig. 7 Schematic summary of the TRα1 and TRβ expression and localization 14 days after a focal ischemic stroke. Areas e1, e2, and e3 correspond to the infarct core and scar, proximal peri-infarct tissue, and contralateral hemisphere, respectively. Macrophages and foam cells are located within e1 and express only nuclear TRα1. Astrocytes mildly (+) express nuclear TRα1 in e1 and e2 areas and a strong (+++) nuclear TRβ within the astrocytic scar. Neurons are mainly TRα1+ (and weakly TRβ+) in all three areas, but close to the infarct (e2 peri-infarct area), more of them exhibit a stronger TRα1 and TRβ signal (mainly nuclear). Oligodendrocytes universally express both TRs in all three areas studied (not illustrated here). These distributions pose different possible effects of the TH over the different cellular populations of the infarcted brain
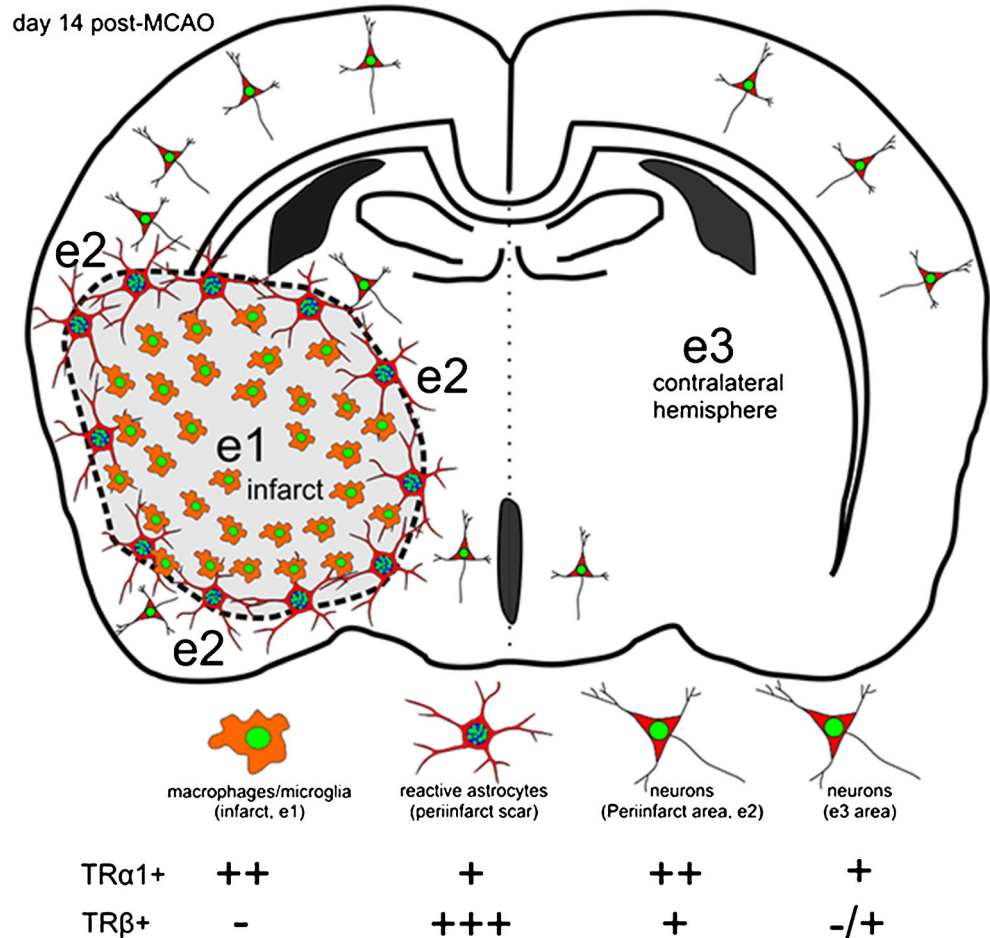

as a combination hypothyroidism, post-stroke inflammation (Iadecola and Anrather 2011), and a probable implication of the orexin pathways (inducing low food intake and reduced mobility) (Lopez et al. 2010; Xiong et al. 2013). In any case, the TH reduction seems to have important implications in the pathophysiology of ischemia and warrants further investigation.

Although TRs are the mediators of TH action, their expression and localization in the infarcted brain remains largely unknown. Despite their importance for the developing

Fig. 8 Confocal 3D study of TRβ expression in the paranodal and juxta-paranodal areas of myelin sheaths. **a** Z-stack confocal 3D image from corpus callosum. **b** Magnification of the selected area in **a**. **c** 3D reconstruction of a single Ranvier node (*asterisk*) with its paranode (*solid arrowheads*) and some of the juxta-paranodal area (*open arrowheads*). TRβ is co-expressed with Caspr in the paranodes and its expression extents 1–2 μm in the juxta-paranodal area. **d** Colocalization output of TRβ and Caspr (*gray*)
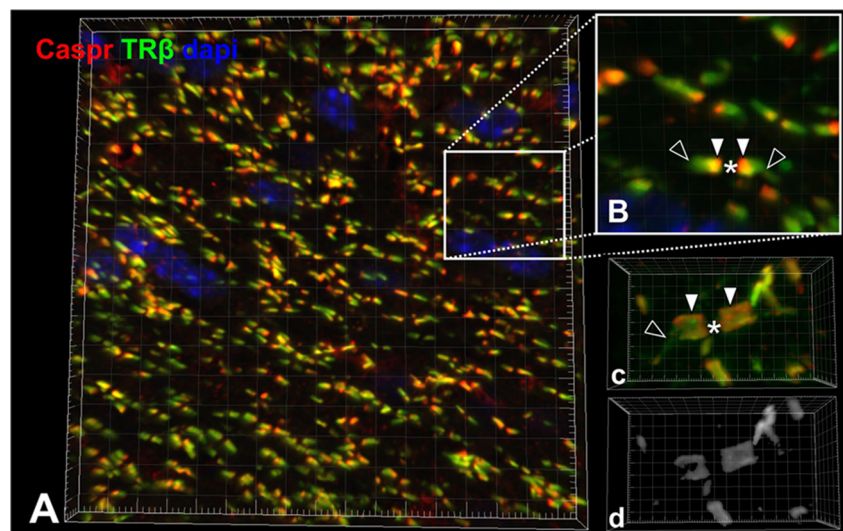
nervous system (Di Liegro 2008), data during the remodeling processes of stroke are lacking. During remodeling (which lasts for several weeks post-ischemia), the peri-infarct zone mimics early developmental stages (a "switch" to developmental conditions) with increased plasticity and permissive microenvironment (Cramer and Chopp 2000; Carmichael 2006; Cramer 2008). It is therefore tempting to speculate that the combination of low TH values along with the specific nuclear expression of TRs resembles embryonic stages, a time where TH/TR balance favors the "apo-receptor" state and during which brain cell numbers increase (Bernal and Morte 2013). Similarly, studies in neonatal cardiomyocytes as well as during post-ischemic cardiac remodeling (Pantos et al. 2012) dictate a possible conserved role for TH signaling in control of the balance between proliferation and differentiation in various organs.

Our WB data show that total TRα1 protein expression is similar to sham-operated animals in all brain areas examined, while TRβ1 is heterogeneously modified in the infarct core (reduced expression) and peri-infarct tissue (possible nuclear translocation). More importantly, neuropathology indicates that TRs' expression derives from different localization as well as different cellular populations. Within the infarction core, neurons are absent and TRα1 expression originates from reactive macrophages/microglia and astrocytes. Around the infarction, neurons are expressing more TRα1 (and to lesser extent TRβ) in their nucleus compared to the healthy hemisphere. This indicates that the TH signaling is more active, suggesting a mechanism of adaptive response under stress as observed in other injury models (Mourouzis et al. 2011; Shulga and Rivera 2013) and TRα1 transgenic animals (Wallis et al. 2008). The lower TR expression in neurons distant from the infarct (contralateral hemisphere), along with diminished nuclear localization, could probably indicate a lower activation of TH signaling in unstressed state. This diversity warrants further studies to identify the exact mechanisms underlying the potential implication of TH in the remodeling/repair processes after cerebral ischemia.

The majority of resting microglia in remote from infarction areas do not express TRα1 or TRβ, while infarction macrophages/microglia are all TRα1+. The latter suggests that the cellular activation state might influence the expression pattern of TRs or vice versa. On one hand, this concept is consistent with evidence suggesting that nuclear receptors and co-repressors (NCoR) can determine the state of microglia and macrophage activation (Ogawa et al. 2004; Saijo et al. 2013). In the case of NCoR particularly, their direct implication with TR function (Astapova and Hollenberg 2013) provides evidence for multiple genomic functions of TH on macrophages/ microglia. On the other hand, TH (in particular T4) seems to antagonize directly members of the proinflammatory macrophage cytokines (MIF) via nongenomic mechanisms, thereby providing a second level of TH control over macrophage

activity (Al-Abed et al. 2011). Furthermore, previous studies have highlighted the role of TH on microglial behavior in the developing brain (Lima et al. 2001) and such an effect could also be present in the post-ischemic "developmental switch." Overall, the observed TRα1 upregulation in macrophages/ microglia after cerebral ischemia needs to be further elucidated.

To our knowledge, we show for the first time that TRs (mainly TRβ and to a lesser degree TRα1) are selectively upregulated in the reactive astrocytes of the glial ischemic scar. Although previous reports have identified that astrocytes express TRα and TRβ subtypes and, therefore, are direct target cells for TH (Manzano et al. 2007), their role in post-lesional astrocytosis has not been—to our knowledge—investigated. Developmental studies indicate that TH promote astrocytic differentiation (Trentin and Moura Neto 1995; Trentin 2006), and recent pharmacological data suggest that T4 administration after blunt brain injury (Tatsumi et al. 2005) or focal ischemia (Genovese et al. 2013) reduces astrocytic proliferation or GFAP expression. In addition, the role of astrocytes in the post-ischemic scar may also extend to a regulation of local T4/T3 levels (via deiodinases) (Courtin et al. 2005); conversely, T4 can control astrocytic glutamate uptake (Mendes-de-Aguiar et al. 2008) or the release of neurotrophic factors (Shulga et al. 2009), both of which can potentially support post-ischemic neurons. Overall, our data suggest that astrocytic post-ischemic functions are probably performed in an environment of high TR expression and low serum TH concentrations (leading to "apo-receptor" state of TRs), although direct proof of brain post-ischemic TH levels is still lacking. In this context, the pharmacological manipulation of TRβ (mainly) and TRα post-ischemia could have important implications for the control of astrocytic functions.

Finally, along with the spatial expression of TRs, we detected for the first time that TRβ is abundantly expressed in the paranodal and juxta-paranodal regions of myelinated axons in the nonischemic tissue. TRβ localization in the paranodal and juxta-paranodal areas of Ranvier nodes could be paired to the reported presence of potassium channels (Kv-KCNQ2 and KCNQ3) that are important for the regulation of repetitive discharges (Devaux et al. 2004; Zoupi et al. 2011). Since TRβ1 but not TRα1 can deactivate other voltage-activated potassium channels (KCNH2 channels) (Storey et al. 2006), our results may suggest a control of the regional potassium channels by TRβ1, which remains to be verified. In addition, the presence of TRβ in the complex of Ranvier nodes could theoretically influence myelin formation, compaction, and function in this specific area. Given the fact that TH in general are considered important to myelination during development (Bernal 2007) or demyelinated CNS disorders (Calza et al. 2010), the TRβ presence in the Ranvier nodes points at possible, undiscovered so far, nongenomic TH actions that may guide or tune the myelination processes.

In conclusion, our study provides experimental evidence for (1) time-specific reductions in TH levels up to day 14 post-stroke; (2) cell-specific, spatial changes in TRs post-ischemia; and (3) TRβ localization in the paranodal and juxta-paranodal areas of Ranvier nodes in the post-ischemic CNS. Further studies should elucidate the precise time kinetics of TRs and thyroid metabolism after stroke and determine the relevant effects and mechanisms on post-stroke remodeling pathology.

Conflict of Interest The authors have nothing to disclose in relevance to the present study.

References

Akhoundi FH, Ghorbani A, Soltani A, Meysamie A (2011) Favorable functional outcomes in acute ischemic stroke patients with subclinical hypothyroidism. Neurology 77:349–354

Al-Abed Y, Metz CN, Cheng KF, Aljabari B, VanPatten S, Blau S et al (2011) Thyroxine is a potential endogenous antagonist of macrophage migration inhibitory factor (MIF) activity. Proc Natl Acad Sci U S A 108:8224–8227

Alevizaki M, Synetou M, Xynos K, Pappa T, Vemmos KN (2007) Low triiodothyronine: a strong predictor of outcome in acute stroke patients. Eur J Clin Investig 37:651–657

Astapova I, Hollenberg AN (2013) The in vivo role of nuclear receptor corepressors in thyroid hormone action. Biochim Biophys Acta 1830:3876–3881

Bernal J (2007) Thyroid hormone receptors in brain development and function. Nat Clin Pract Endocrinol Metab 3:249–259

Bernal J, Morte B (2013) Thyroid hormone receptor activity in the absence of ligand: physiological and developmental implications. Biochim Biophys Acta 1830(7):3893–3899

Boelen A, Kwakkel J, Fliers E (2011) Beyond low plasma T3: local thyroid hormone metabolism during inflammation and infection. Endocr Rev 32:670–693

Calza L, Fernandez M, Giardino L (2010) Cellular approaches to central nervous system remyelination stimulation: thyroid hormone to promote myelin repair via endogenous stem and precursor cells. J Mol Endocrinol 44:13–23

Carmichael ST (2006) Cellular and molecular mechanisms of neural repair after stroke: making waves. Ann Neurol 59:735–742

Chassande O (2003) Do unliganded thyroid hormone receptors have physiological functions? J Mol Endocrinol 31:9–20

Courtin F, Zrouri H, Lamirand A, Li WW, Mercier G, Schumacher M et al (2005) Thyroid hormone deiodinases in the central and peripheral nervous system. Thyroid 15:931–942

Cramer SC (2008) Repairing the human brain after stroke: I. Mechanisms of spontaneous recovery. Ann Neurol 63:272–287

Cramer SC, Chopp M (2000) Recovery recapitulates ontogeny. Trends Neurosci 23:265–271

Devaux JJ, Kleopa KA, Cooper EC, Scherer SS (2004) KCNQ2 is a nodal K + channel. J Neurosci 24:1236–1244

Di Liegro I (2008) Thyroid hormones and the central nervous system of mammals (review). Mol Med Rep 1:279–295

Diano S, Horvath TL (2008) Type 3 deiodinase in hypoxia: to cool or to kill? Cell Metab 7:363–364

Dittmar M, Spruss T, Schuierer G, Horn M (2003) External carotid artery territory ischemia impairs outcome in the endovascular filament model of middle cerebral artery occlusion in rats. Stroke 34:2252–2257

Dittmar MS, Vatankhah B, Fehm NP, Retzl G, Schuierer G, Bogdahn U et al (2005) The role of ECA transection in the development of masticatory lesions in the MCAO filament model. Exp Neurol 195:372–378

Genovese T, Impellizzeri D, Ahmad A, Cornelius C, Campolo M, Cuzzocrea S et al (2013) Post-ischaemic thyroid hormone treatment in a rat model of acute stroke. Brain Res 1513:92–102

Golombek SG (2008) Nonthyroidal illness syndrome and euthyroid sick syndrome in intensive care patients. Semin Perinatol 32:413–418

Harada H, Wang Y, Mishima Y, Uehara N, Makaya T, Kano T (2005) A novel method of detecting rCBF with laser-Doppler flowmetry without cranial window through the skull for a MCAO rat model. Brain Res Brain Res Protoc 14:165–170

Hung PL, Huang CC, Huang HM, Tu DG, Chang YC (2013) Thyroxin treatment protects against white matter injury in the immature brain via brain-derived neurotrophic factor. Stroke 44:2275–2283

Iadecola C, Anrather J (2011) The immunology of stroke: from mechanisms to translation. Nat Med 17:796–808

Lee CH, Yoo KY, Hwang IK, Choi JH, Park OK, Li H et al (2010) Hypothyroid state does not protect but delays neuronal death in the hippocampal CA1 region following transient cerebral ischemia: focus on oxidative stress and gliosis. J Neurosci Res 88:2661–2668

Lima FR, Gervais A, Colin C, Izembart M, Neto VM, Mallat M (2001) Regulation of microglial development: a novel role for thyroid hormone. J Neurosci 21:2028–2038

Lopez M, Tena-Sempere M, Dieguez C (2010) Cross-talk between orexins (hypocretins) and the neuroendocrine axes (hypothalamic-pituitary axes). Front Neuroendocrinol 31:113–127

Lourbopoulos A, Karacostas D, Artemis N, Milonas I, Grigoriadis N (2008) Effectiveness of a new modified intraluminal suture for temporary middle cerebral artery occlusion in rats of various weight. J Neurosci Methods 173:225–234

Lourbopoulos A, Chatzigeorgiou S, Mavridis T, Kokkinakis I, Tascos N, Simeonidou C (2012) Stereotactic coordinates for intracerebroventricular infusion after permanent focal cerebral ischemia in Wistar rats. Hippokratia 16:51–56

Manzano J, Bernal J, Morte B (2007) Influence of thyroid hormones on maturation of rat cerebellar astrocytes. Int J Dev Neurosci 25:171–179

Mendes-de-Aguiar CB, Alchini R, Decker H, Alvarez-Silva M, Tasca CI, Trentin AG (2008) Thyroid hormone increases astrocytic glutamate uptake and protects astrocytes and neurons against glutamate toxicity. J Neurosci Res 86:3117–3125

Mistry N, Wass J, Turner MR (2009) When to consider thyroid dysfunction in the neurology clinic. Pract Neurol 9:145–156

Mourouzis I, Forini F, Pantos C, Iervasi G (2011) Thyroid hormone and cardiac disease: from basic concepts to clinical application. J Thyroid Res 2011:958626

Ogawa S, Lozach J, Jepsen K, Sawka-Verhelle D, Perissi V, Sasik R et al (2004) A nuclear receptor corepressor transcriptional checkpoint controlling activator protein 1-dependent gene networks required for macrophage activation. Proc Natl Acad Sci U S A 101:14461–14466

Pantos C, Mourouzis I, Saranteas T, Paizis I, Xinaris C, Malliopoulou V et al (2005) Thyroid hormone receptors alpha1 and beta1 are downregulated in the post-infarcted rat heart: consequences on the response to ischaemia-reperfusion. Basic Res Cardiol 100:422–432

Pantos C, Mourouzis I, Galanopoulos G, Gavra M, Perimenis P, Spanou D et al (2010) Thyroid hormone receptor alpha1 downregulation in postischemic heart failure progression: the potential role of tissue hypothyroidism. Horm Metab Res 42:718–724

Pantos C, Mourouzis I, Cokkinos DV (2012) Thyroid hormone and cardiac repair/regeneration: from Prometheus myth to reality? Can J Physiol Pharmacol 90(8):977–987

Portella AC, Carvalho F, Faustino L, Wondisford FE, Ortiga-Carvalho TM, Gomes FC (2010) Thyroid hormone receptor beta mutation causes severe impairment of cerebellar development. Mol Cell Neurosci 44:68–77

Puymirat J, Miehe M, Marchand R, Sarlieve L, Dussault JH (1991) Immunocytochemical localization of thyroid hormone receptors in the adult rat brain. Thyroid 1:173–184

Rogers DC, Campbell CA, Stretton JL, Mackay KB (1997) Correlation between motor impairment and infarct volume after permanent and transient middle cerebral artery occlusion in the rat. Stroke 28:2060–2065, discussion 2066

Saijo K, Crotti A, Glass CK (2013) Regulation of microglia activation and deactivation by nuclear receptors. Glia 61:104–111

Shulga A, Rivera C (2013) Interplay between thyroxin, BDNF and GABA in injured neurons. Neuroscience 239:241–252

Shulga A, Blaesse A, Kysenius K, Huttunen HJ, Tanhuanpaa K, Saarma M et al (2009) Thyroxin regulates BDNF expression to promote survival of injured neurons. Mol Cell Neurosci 42:408–418

Simonides WS, Mulcahey MA, Redout EM, Muller A, Zuidwijk MJ, Visser TJ et al (2008) Hypoxia-inducible factor induces local thyroid hormone inactivation during hypoxic-ischemic disease in rats. J Clin Invest 118:975–983

Storey NM, Gentile S, Ullah H, Russo A, Muessel M, Erxleben C et al (2006) Rapid signaling at the plasma membrane by a nuclear receptor for thyroid hormone. Proc Natl Acad Sci U S A 103:5197–5201

Tatsumi K, Haga S, Matsuyoshi H, Inoue M, Manabe T, Makinodan M et al (2005) Characterization of cells with proliferative activity after a brain injury. Neurochem Int 46:381–389

Theotokis P, Lourbopoulos A, Touloumi O, Lagoudaki R, Kofidou E, Nousiopoulou E et al (2012) Time course and spatial profile of Nogo-A expression in experimental autoimmune encephalomyelitis in C57BL/6 mice. J Neuropathol Exp Neurol 71:907–920

Trentin AG (2006) Thyroid hormone and astrocyte morphogenesis. J Endocrinol 189:189–197

Trentin AG, Moura Neto V (1995) T3 affects cerebellar astrocyte proliferation, GFAP and fibronectin organization. Neuroreport 6:293–296

Vose LR, Vinukonda G, Jo S, Miry O, Diamond D, Korumilli R et al (2013) Treatment with thyroxine restores myelination and clinical recovery after intraventricular hemorrhage. J Neurosci 33:17232–17246

Wallis K, Sjogren M, van Hogerlinden M, Silberberg G, Fisahn A, Nordstrom K et al (2008) Locomotor deficiencies and aberrant development of subtype-specific GABAergic interneurons caused by an unliganded thyroid hormone receptor alpha1. J Neurosci 28:1904–1915

Wallis K, Dudazy S, van Hogerlinden M, Nordstrom K, Mittag J, Vennstrom B (2010) The thyroid hormone receptor alpha1 protein is expressed in embryonic postmitotic neurons and persists in most adult neurons. Mol Endocrinol 24:1904–1916

Williams AJ, O'Shea PJ, Williams GR (2007) Complex interactions between thyroid hormone and fibroblast growth factor signalling. Curr Opin Endocrinol Diabetes Obes 14:410–415

Wollenweber FA, Zietemann V, Gschwendtner A, Opherk C, Dichgans M (2013) Subclinical hyperthyroidism is a risk factor for poor functional outcome after ischemic stroke. Stroke 44:1446–1448

Xiong X, White RE, Xu L, Yang L, Sun X, Zou B et al (2013) Mitigation of murine focal cerebral ischemia by the hypocretin/orexin system is associated with reduced inflammation. Stroke 44:764–770

Zhang Y, Meyer MA (2010) Clinical analysis on alteration of thyroid hormones in the serum of patients with acute ischemic stroke. Stroke Res Treat 2010:290678

Zhang Z, Zhang L, Yepes M, Jiang Q, Li Q, Arniego P et al (2002) Adjuvant treatment with neuroserpin increases the therapeutic window for tissue-type plasminogen activator administration in a rat model of embolic stroke. Circulation 106:740–745

Zoupi L, Savvaki M, Karagogeos D (2011) Axons and myelinating glia: an intimate contact. IUBMB Life 63:730–735